

Design and Analysis of Compact Single and Dual Notch Ultra Wideband Bandpass Filter

Madhu Gandamalla*, Dushyant Marathe, and Kishore Kulat

Abstract—This paper presents single and dual notch ultra-wideband bandpass filters (UWB BPFs) to mitigate interference with coexisting wireless communication systems in ultra-wideband (UWB). The single and dual notch UWB BPF is developed by using signal interaction concept loaded with stub loaded resonator. The stub loaded resonator creates notches in the passband to avoid the interference with coexisting wireless communication systems. The notch frequency can be placed at the points of interest within passband by selecting a proper length of stub loaded resonator. Transmission zeros are introduced to enhance the selectivity of stopband. It presents UWB BPF with single notch at the frequency of 6.5 GHz and dual notch at the frequencies of 6.3 GHz and 8.0 GHz. The circuit size of proposed filters is $6\text{ mm} \times 6\text{ mm}$ and $6\text{ mm} \times 6\text{ mm}$. The proposed filters exhibit good performance in terms of compact size, good fractional bandwidth and sharp selectivity. All the filters are simulated and fabricated on a Rogers R03010 substrate with relative permittivity of 10.2 and thickness of 1.28 mm. There is good agreement between simulated and measured results.

1. INTRODUCTION

Filters are key elements in the microwave wireless communication systems. They are used to pass or stop different frequencies. Filters are used for the design of Impedance matching networks, time delay networks and slow wave structures [1]. The negative resistance amplifiers utilise filter structures for the optimum broadband operation [1]. Ultra-wideband (UWB) is a wireless communication technology which transfers extremely large amount of data over a wide bandwidth. Unlike other communication technologies, UWB uses short signal pulses to transmit information over a broad spectrum with low power. The frequency range of UWB is from 3.1 to 10.6 GHz, and it was authorised by Federal communications commission (FCC) in 2002 for indoor applications [2]. UWB systems offer high data rates, high precision for location and imaging devices, and high resolution for sensing devices. UWB devices find applications in radar, imaging and military communications [3]. UWB devices also have many applications in home networking and multimedia communications in the form of Wireless Personal Area Network (WPAN).

The interference with coexisting wireless communication systems can degrade the performance of UWB systems. The challenging task of UWB is to eliminate the interference with coexisting wireless communication systems. The coexisting communication systems are WLAN, WiMAX and satellite communication systems, and the operating frequencies are 5.2–5.8 GHz, 3.5 GHz and 8.0 GHz [4]. To eliminate interference with coexisting wireless communication systems, ultra-wideband band pass filters (BPFs) with notches are designed. In context, several approaches have been proposed to design UWB BPF with notches. In [5], the UWB BPF with notches is designed by using a short and open circuited stub loaded resonator to eliminate interference from WLAN and satellite communication. The dual

Received 7 August 2018, Accepted 18 October 2018, Scheduled 1 November 2018

* Corresponding author: Madhu Gandamalla (madhuxolo@gmail.com).

The authors are with the Department of Electronics and Communication Engineering, Visvesvaraya National Institute of Technology (VNIT), Nagpur, India.

notches are realised by using inward folded resonator and spiral resonators [5]. The filter exhibits high selectivity and good return loss. Balanced UWB BPF with notches is developed based on triple mode slotline resonators and differential microstrip slotline transitions. Dual notched bands are designed by using inverse QWRs coupling stepped impedance microstrip stub loaded in 50 ohm microstrip feed lines [6]. A stepped impedance slotline multimode resonator with microstrip to slotline transitions is used to develop balanced single notch based UWB BPF. The filter eliminates WLAN signal [7]. Using transversal signal interaction concept, the UWB BPF with notch is designed [8]. Previously reported filters have large size and small fractional bandwidth. The proposed filters exhibit good selectivity, small size and good fractional bandwidth.

In this paper, single and dual notch UWB BPFs are developed by using signal interaction concept loaded with an open circuited stub resonator using microstrip technology. The signal interaction concept utilises four quarter wavelength resonators to develop UWB passband. The stub loaded resonator introduces notches in UWB passband to avoid interference with WLAN and satellite communication. The proposed single notch UWB BPF contains a notch at the frequency of 6.5 GHz and dual notch UWB BPF contains notches at the frequencies of 6.3 GHz and 8.0 GHz. All the filters are simulated, fabricated and measured.

2. DESIGN OF PROPOSED UWB BPF

Figure 1 depicts the topology of proposed circuit which consists of two parallel transmission paths. Each transmission path has two quarter wavelength resonators. The proposed circuit of UWB BPF contains a short circuit exactly at the centre of the first transmission path. The characteristic impedance of ports is 50 ohm. Z_1 represents the characteristic impedance of resonator, and θ_1 is the electrical length of corresponding resonator.

2.1. Analysis of Proposed Circuit

The proposed network depicted in Figure 1 is a symmetric network, and even/odd mode analysis can be used to analyse the proposed circuit. After applying even mode signals to the two-port symmetric network, the line of symmetry becomes an open circuit, and two-port network becomes two one-port, even mode networks which are identical. Similarly, after applying odd mode signals to the two-port symmetric network, the line of symmetry becomes a short circuit, and the two-port network becomes two one-port, odd mode networks which are identical [9]. The even mode and odd mode equivalent circuits are shown in Figure 2.

The input admittances for the even mode equivalent circuit and odd mode equivalent circuit are given by Y_{ine} and Y_{ino} , where y_0 represents the characteristic admittance of port.

$$Y_{ine} = -\frac{j \cot[\theta_1]}{z_1} + \frac{j \tan[\theta_1]}{z_1} \quad (1)$$

$$Y_{ino} = -\frac{2j \cot[\theta_1]}{z_1} \quad (2)$$

$$S_{11} = \frac{1}{2} y_0 z_1 \left(\frac{1}{-4j \cot[\theta_1] + y_0 z_1} + \frac{j \cot[\theta_1]}{-2 + 2 \cot[\theta_1]^2 + j \cot[\theta_1] y_0 z_1} \right) \quad (3)$$

$$S_{21} = \frac{j \csc[\theta_1]^2 y_0 z_1}{(4 \cot[\theta_1] + j y_0 z_1)(-2 + 2 \cot[\theta_1]^2 + j \cot[\theta_1] y_0 z_1)} \quad (4)$$

The odd mode and even mode resonant frequencies can be determined by equating Y_{ine} and Y_{ino} to zero. So,

$$Y_{ine} = 0 \Rightarrow \tan[\theta_1] = \cot[\theta_1] \quad (5)$$

$$Y_{ino} = 0 \Rightarrow \cot[\theta_1] = 0 \quad (6)$$

The above condition in Eq. (5) is satisfied when $\theta_1 = (2n + 1)\frac{\pi}{4}$; this implies that the proposed circuit resonates at even mode frequencies when the electrical length of a resonator is odd multiples of 45 degrees. Figure 3 shows the variation of even mode input admittance with respect to electrical length

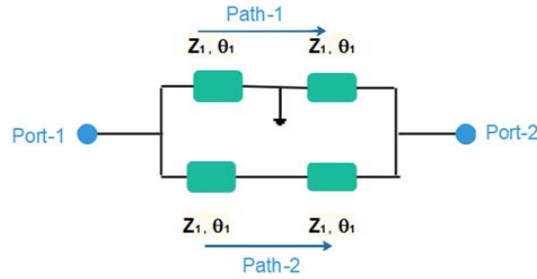


Figure 1. Topology of proposed UWB BPF circuit.



Figure 2. (a) Equivalent even mode circuit of proposed UWB BPF. (b) Equivalent odd mode circuit of proposed UWB BPF.

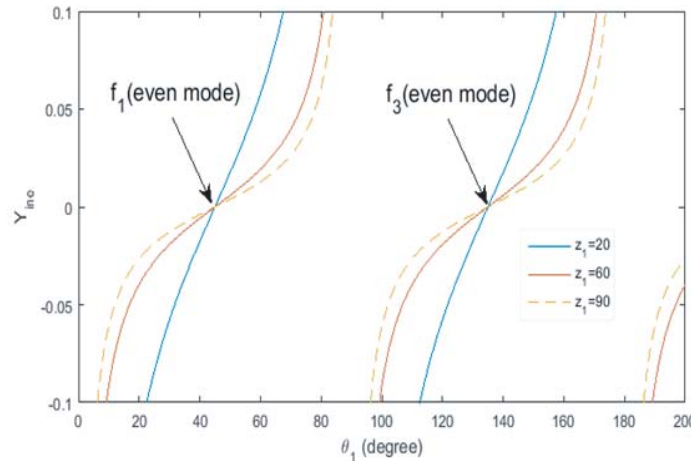


Figure 3. Variation of even mode input admittance of proposed UWB BPF against electrical length (θ_1).

(θ_1), for various values of characteristic impedance (Z_1). The frequencies f_1 and f_3 are even mode resonant frequencies.

The above condition in Eq. (6) is satisfied when $\theta_1 = (2n + 1)\frac{\pi}{2}$; this implies that the proposed circuit resonates at odd mode frequencies when the electrical length (θ_1) of a resonator is odd multiples of 90 degrees. Figure 4 shows the variation of odd mode input admittance with respect to electrical length (θ_1), for various values of characteristic impedance (Z_1). The frequency f_2 is odd mode resonant frequency.

The transmission zeros of a proposed circuit can be obtained by equating the magnitude of transmission coefficient to zero.

$$|S_{21}| = 0 \Rightarrow \tan[\theta_1] = 0 \tag{7}$$

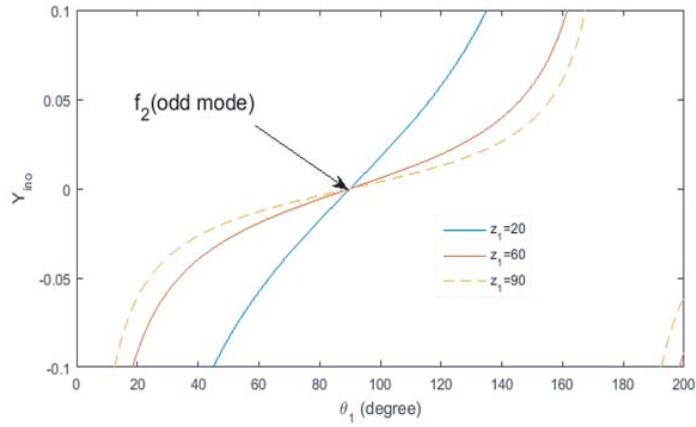


Figure 4. Variation of odd mode input admittance of proposed UWB BPF against electrical length (θ_1).

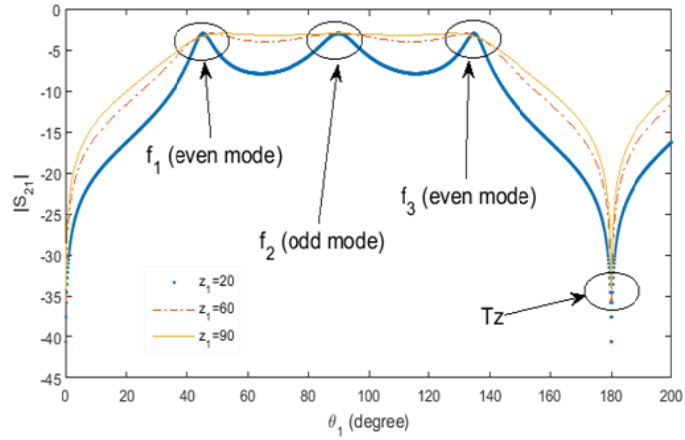


Figure 5. Variation of $|S_{21}|$ (dB) against electrical length (θ_1).

The above condition in Eq. (7) is satisfied when $\theta_1 = n\pi$; this implies that the proposed circuit has transmission zeros (Tz) at frequencies when the electrical length of resonator is integer multiple of 180 degrees, where n is an integer and $n = 0, 1, 2, 3, \dots$

Figure 5 shows the variation of magnitude of transmission coefficient from port 1 to port 2 with respect to electrical length (θ_1), for various values of characteristic impedance (Z_1). The bandwidth of the proposed circuit can be formed by the three resonant frequencies namely f_1 , f_2 and f_3 . Among them f_1, f_3 are the even mode resonant frequencies, and f_2 is the odd mode resonant frequency. The electrical lengths of frequencies f_1 , f_2 and f_3 are 45° , 90° and 135° . The transmission zero occurs at frequency where the electrical length is 180° . The position of transmission zero can be varied by changing the physical length of resonator.

The realisation of proposed theory is shown in Figure 6(a). The top view of the proposed circuit is illustrated in Figure 6(a), and resonators are placed in circular fashion. The short circuit is present at the centre of first transmission path and has 0.25 mm radius. The transmission zeros occur when the signals from two parallel transmission paths get canceled out. The length and width of the resonator are chosen to be 4.71 mm and 0.8 mm (which is equal to 60 ohm characteristic impedance). The length (fl) and width (fw) of a feed line are 5.96 mm and 1.2 mm (which is equal to 50 ohm characteristic impedance). All the lengths are calculated at the resonant frequency of 6.1 GHz and characteristic impedance of ports chosen to be 50 ohm. The proposed filter is simulated by using Ansoft HFSS

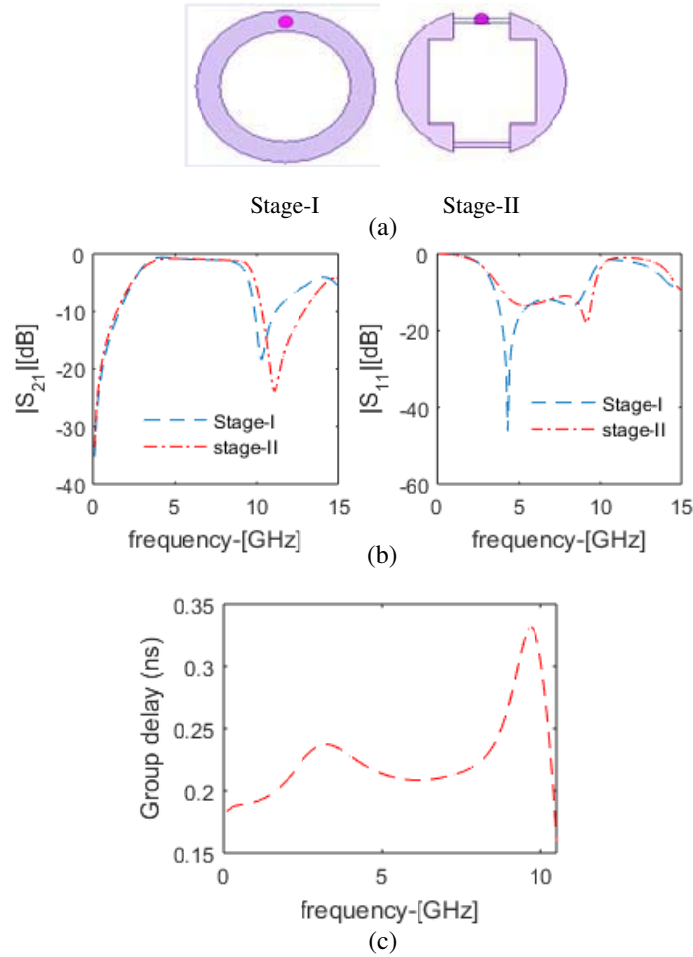


Figure 6. (a) Top view of various stages of proposed UWB BPF. (b) S -parameter (dB) response of Stage-I and Stage-II of proposed UWB BPF. (c) Group delay of the proposed UWB BPF.

software on the substrate Rogers R03010 which has relative permittivity of 10.2 and substrate thickness of 1.28 mm. Stage-I filter is transformed to stage-II filter to enhance the performance. S parameter response of stage-I and stage-II is shown in Figure 6(b). Stage-II filter is an UWB BPF and covers the 3-dB frequency band from 2.87 GHz to 9.68 GHz. UWB BPF possesses 3-dB fractional bandwidth (FBW) of 111.6%. Figure 6(c) illustrates the group delay of the proposed UWB BPF, which is less than 0.35 ns within the passband.

3. DESIGN OF PROPOSED STUB LOADED RESONATOR

Figure 7 depicts the topology of stub-loaded resonator which consists of two identical resonators on either side with characteristic impedance of Z_2 and electrical length of θ_2 . One open stub is loaded at middle which has characteristic impedance of Z_2 and electrical length of θ_3 . Especially, the proposed stub loaded resonator is created to insert notches in the passband of UWB BPF. For symmetrical network, even/odd mode analysis can be used to analyse the circuit.

3.1. Even/Odd Mode Analysis

Figure 8 illustrates the even and odd mode equivalent circuits of stub-loaded resonator. The even mode and odd mode input admittances of the stub-loaded resonator are given by \mathbf{Y}_{ine} and \mathbf{Y}_{ino} . The odd

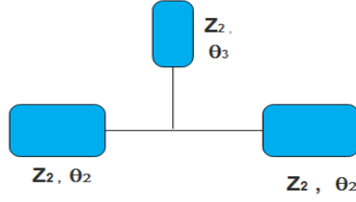


Figure 7. Topology of proposed stub loaded resonator.

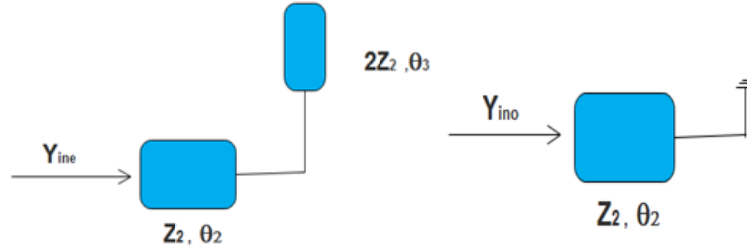


Figure 8. Even/odd equivalent circuits of proposed stub loaded resonator.

mode and even mode resonant frequencies can be obtained by equating Y_{ine} and Y_{ino} to zero.

$$Y_{ine} = \frac{\text{Cos}[\theta_2] + 2 \cot[\theta_3] \text{Sin}[\theta_2]}{-2jZ_2 \text{Cos}[\theta_2] \cot[\theta_3] + jZ_2 \text{Sin}[\theta_2]} \quad (8)$$

$$Y_{ine} = 0 \quad (9)$$

$$Y_{ino} = -\frac{j \text{Cot}[\theta_2]}{Z_2} \quad (10)$$

$$Y_{ino} = 0 \Rightarrow \text{Cot}[\theta_2] = 0 \quad (11)$$

The above condition in Eq. (11) is satisfied when $\theta_2 = (2n + 1)\frac{\pi}{2}$; this implies that the proposed circuit resonates at odd mode frequencies when the electrical length (θ_2) of a resonator is odd multiples of 90 degrees.

Figure 9 shows the variation of input even mode admittance of a stub-loaded resonator against θ_2 . It is clear from Figure 9 that the even mode resonant frequency decreases when θ_2 increases, and for $\theta_2 = 15^\circ$, 45° and 75° , the even mode resonant frequency occurs at the frequency when $\theta_3 = 88^\circ$, 71° and 43° . For $\theta_2 = 90^\circ$, the even mode resonant frequency occurs at the frequency when $\theta_3 = 20^\circ$. Hence, the even mode resonant frequency can be placed at the points of interest by selecting proper value of θ_2 .

Figure 10 shows the variation of input even mode admittance of a stub-loaded resonator against θ_3 . It is clear from Figure 10 that the even mode resonant frequency decreases when θ_3 increases, and for $\theta_3 = 4^\circ$, the even mode resonant frequency occurs at the frequency when $\theta_2 = -2^\circ$ and 178° . For $\theta_3 = 34^\circ$, the even mode resonant frequency occurs at the frequency when $\theta_2 = -19^\circ$ and 161° . For $\theta_3 = 62^\circ$, the even mode resonant frequency occurs at the frequency when $\theta_2 = -43^\circ$ and 137° . For $\theta_3 = 90^\circ$, the even mode resonant frequency occurs at the frequency when $\theta_2 = 90^\circ$. For $90^\circ \geq \theta_3 \geq 4^\circ$ and θ_2 is fixed, the proposed stub-loaded resonator introduces two even mode resonant frequencies, and otherwise, it creates one even mode resonant frequency. Hence, the two even mode resonant frequencies can be placed at the points of interest by selecting a proper value of θ_3 .

4. DESIGN OF SINGLE AND DUAL NOTCH UWB BPF

The UWB BPFs with single and dual notches are designed by placing the stub-loaded resonator in the UWB BPF. The even mode resonant frequency of the proposed stub-loaded resonator eliminates the interference with coexisting wireless communication systems in UWB. For a single notch UWB BPF,

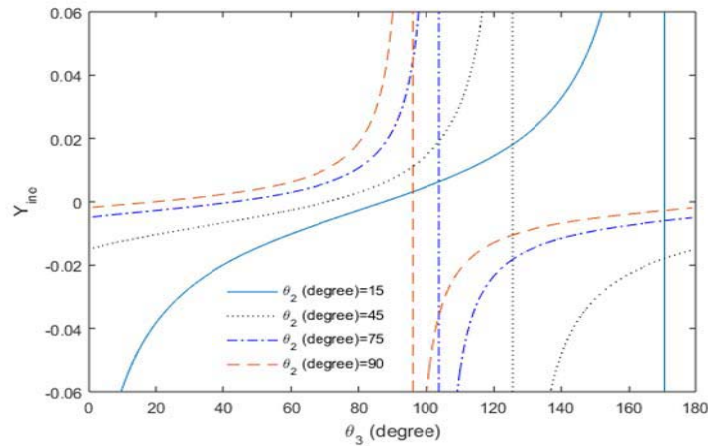


Figure 9. Variation of even mode input admittance of proposed stub load resonator against θ_2 .

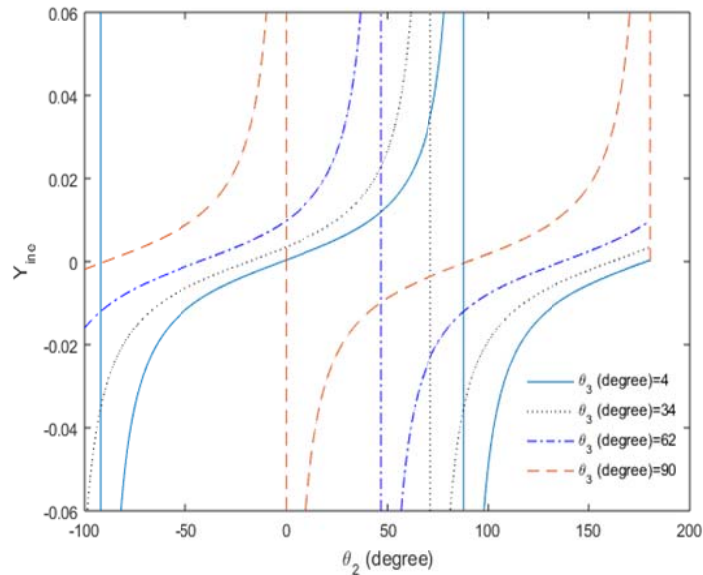


Figure 10. Variation of even mode input admittance of proposed stub load resonator against θ_3 .

the electrical lengths $\theta_1 = 90^\circ$, $\theta_2 = 90^\circ$ and $\theta_3 = 3.6^\circ$ are chosen, and its corresponding physical lengths are 4.95 mm, 4.95 mm and 0.2 mm. The characteristic impedance (Z_2) of stub-loaded resonator is chosen to be 95.46 ohm, and its corresponding width is 0.2 mm. The even mode resonant frequency of stub-loaded resonator creates a notch in the UWB BPF passband. Figure 11(a) illustrates the layout of the single notch UWB BPF. The physical dimensions of single notch UWB BPF are $K_1 = 3.2$ mm, $K_2 = 0.2$ mm, $K_3 = 3.4$ mm, $K_4 = 2$ mm, $K_5 = 0.9$ mm, $K_6 = 0.2$ mm, $K_7 = 1.12$ mm, $K_8 = 0.3$ mm, $K_9 = 0.5$ mm, $rw = 0.2$ mm, $R_1 = 3$ mm, $fl = 5.96$ mm, $fw = 1.2$ mm and $m = 3.5$ mm.

For dual notch UWB BPF, the electrical lengths: $\theta_1 = 90^\circ$, $\theta_2 = 90^\circ$ and $\theta_3 = 62^\circ$ are chosen, and its corresponding physical lengths are 4.95 mm, 4.95 mm and 3.4 mm. The characteristic impedance (Z_2) of stub-loaded resonator is chosen to be 95.46 ohm, and its corresponding width is 0.2 mm. The two even mode resonant frequencies of stub-loaded resonator create notches in the UWB BPF passband. Figure 11(b) depicts the layout of dual notch UWB BPF. The length (fl) and width (fw) of a feedline are 5.96 and 1.2 mm. The pink colour filled circle is short circuit which has the radius of 0.25 mm. All the lengths are calculated at the centre frequency of 6.1 GHz. The physical dimensions of dual notch

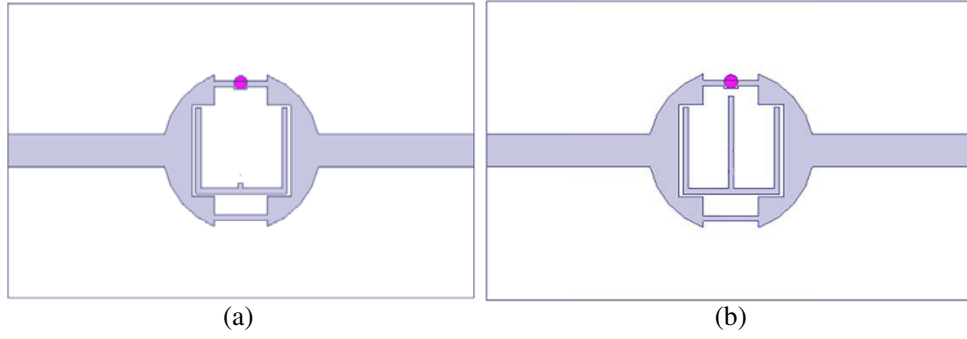


Figure 11. (a) Layout of proposed single notch UWB BPF. (b) Layout of proposed dual notch UWB BPF.

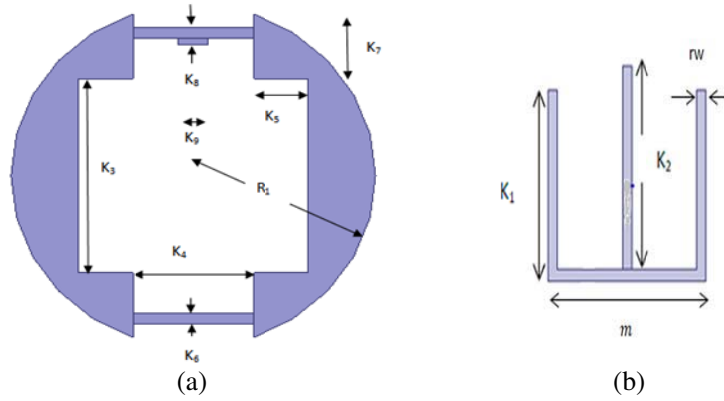


Figure 12. (a) and (b) zoomed view of proposed UWB BPF with notches.

UWB BPF are $K_1 = 3.2$ mm, $K_2 = 3.4$ mm, $K_3 = 3.4$ mm, $K_4 = 2$ mm, $K_5 = 0.9$ mm, $K_6 = 0.2$ mm, $K_7 = 1.12$ mm, $K_8 = 0.3$ mm, $K_9 = 0.5$ mm, $rw = 0.2$ mm, $R_1 = 3$ mm, $fl = 5.96$ mm, $fw = 1.2$ mm and $m = 3.5$ mm.

Figure 12 is zoomed out to show proper physical dimensions of the proposed UWB BPF with single and dual notches. With respect to physical dimension, there is a difference in K_2 value for single and dual notch based UWB BPFs.

4.1. Parametric Analysis

Figure 13(a) illustrates the variation of magnitude of S_{21} with respect to θ_2 for a fixed θ_3 . The electrical length θ_2 accounts for the shift in notch frequency. As θ_2 increases, the notch frequencies decrease for single notch and dual notch UWB BPFs. There is flexibility to place the notch at the points of interest to avoid WLAN interference (single notch) and WLAN, satellite systems interference (dual notches) by varying the electrical length θ_2 . Among all values of θ_2 , $\theta_2 = 90^\circ$ is chosen for both single notch and dual notch UWB BPFs. Figure 13(b) illustrates the variation of magnitude of S_{21} with respect to θ_3 for a fixed θ_2 . The electrical length θ_3 accounts for the creation of the second notch in the passband depending on the value of θ_3 . The value of θ_3 is 3.6° for single notch UWB BPF and 62° for dual notch UWB BPF.

5. EXPERIMENTAL RESULTS

The solid line in Figure 15 shows the measured results of proposed single notch UWB BPF. The proposed single notch UWB BPF covers the passband from 2.945 GHz to 9.7 GHz, and the single notch

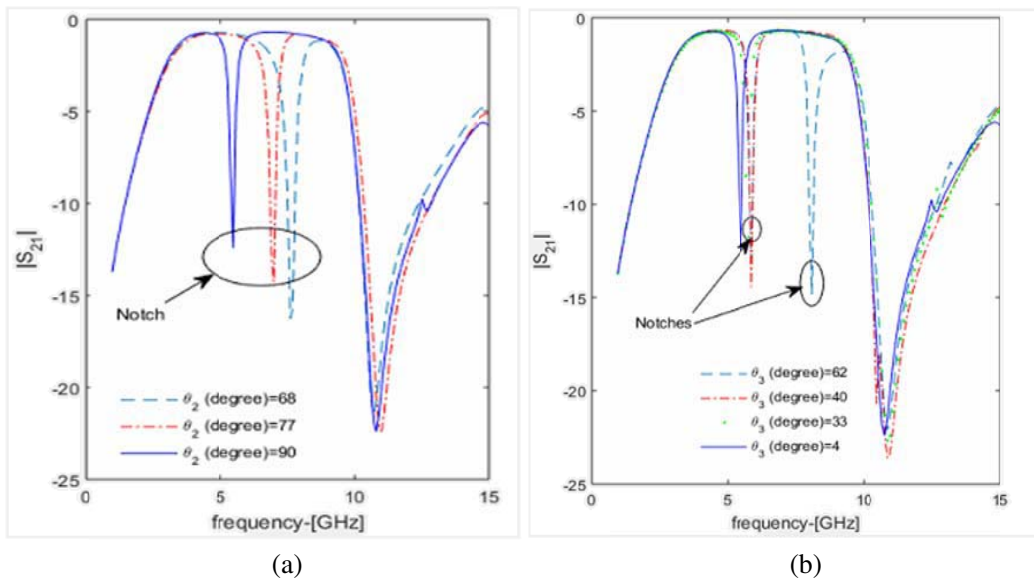


Figure 13. (a) Variation of $|S_{21}|$ (dB) against θ_2 . (b) Variation of $|S_{21}|$ (dB) against θ_3 .

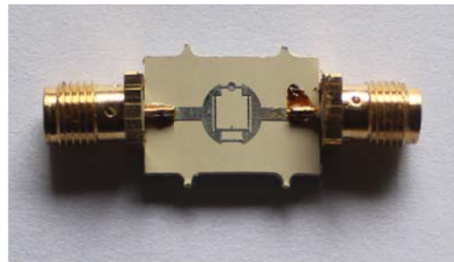


Figure 14. Photograph of fabricated single notch UWB BPF.

is observed at the frequency 6.5 GHz. To avoid the interference from the WLAN communication systems, notch frequency can be shifted in the frequency range of 5.2–5.8 GHz by selecting a proper value of θ_2 . The depth of notch is about greater than 10 dB. Transmission zeros are introduced to enhance the selectivity of upper stopband. One transmission zero is observed at the frequency of 12.9 GHz in the upper stopband. The upper stopband attenuation is greater than 18 dB up to 13.2 GHz. The return loss is greater than 10 dB, and insertion loss is less than 1 dB within the passbands. Figure 14 shows a photograph of the fabricated single notch UWB BPF. The circuit size of the proposed single notch UWB BPF is $6 \times 6 \text{ mm}^2$. Table 1 shows comparison between the proposed filter and some reported single notch UWB bandpass filters. The proposed single notch UWB BPF shows good performance in terms of compact size and sharp selectivity.

The solid line in Figure 17 shows the measured results of the proposed dual notch UWB BPF. The proposed dual notch UWB BPF covers the passband from 2.82 GHz to 9.64 GHz, and dual notches are observed at the frequencies 6.3 GHz and 8 GHz. To avoid the interference from the WLAN and satellite communication systems, notch frequency can be shifted by selecting a proper value of θ_2 . The depths of notches are about greater than 10 dB. One transmission zero is observed at the frequency of 12.9 GHz in the upper stopband. The upper stopband attenuation is greater than 18 dB up to 13.2 GHz. The return loss is greater than 10 dB, and insertion loss is less than 1 dB within the passbands. Figure 16 shows a photograph of the fabricated dual notch UWB BPF. The circuit size of the proposed dual notch UWB BPF is $6 \times 6 \text{ mm}^2$. Table 2 shows the comparison between the proposed filter and some reported dual notch UWB bandpass filters. The proposed dual notch UWB BPF shows good performance in terms

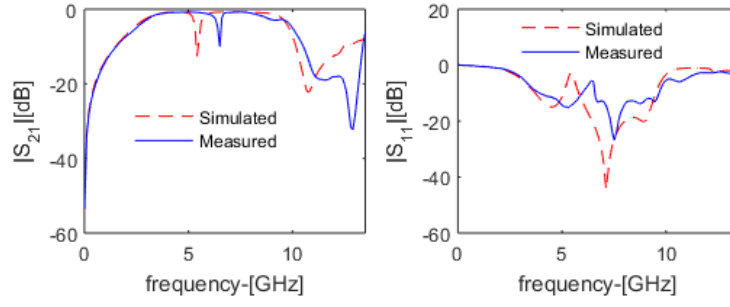


Figure 15. Comparison of measured and simulated results of proposed single notch UWB BPF.

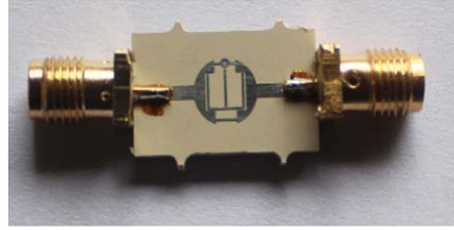


Figure 16. Photograph of fabricated dual notch UWB BPF.

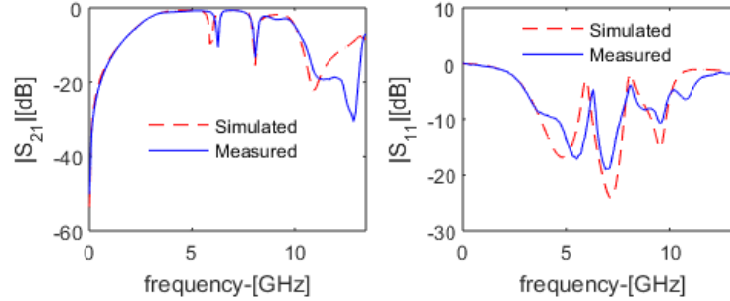


Figure 17. Comparison of measured and simulated results of proposed dual notch UWB BPF.

Table 1. Comparison of proposed single notch UWB BPF with previously reported filters.

Ref	Notch (GHz)	3-dB FBW (%)	Circuit size (λ_q^2)
[10]	5.25–5.5	104	0.69×0.56
[11]	7	103	0.74×0.4
[12]	8.05	110	0.51×0.32
[13]	8.05	116.78	0.56×0.6
[14]	5.8	113	0.87×0.66
This work	6.5	110.7	0.31×0.31

of compact size and sharp selectivity. Group delay variation of single and dual notch UWB BPFs is shown in Figure 18, and the variation is flat within the passband. For single notch UWB BPF, the group delay is less than 0.6 ns within passband. For dual notch UWB BPF, the group delay is less than 0.7 ns within passband.

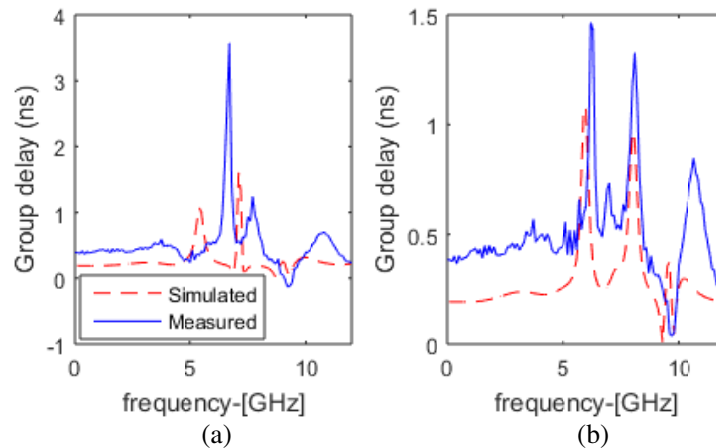


Figure 18. Group delay. (a) Single notch UWB BPF. (b) Dual notch UWB BPF.

Table 2. Comparison of proposed dual notch UWB BPF with previously reported filters.

Ref	Notch (GHz)	3-dB FBW (%)	IL (dB)	Circuit size (λ_g^2)	Suppression (dB)
[15]	5.3/7.8	118	< 2	1.0×0.54	15
[16]	5.23/5.81	N/A	< 1.49	0.359×0.462	20
[17]	5.75/8.05	108	< 2	0.687×0.312	20
[18]	5.9/8	110.7	N/A	0.928×0.451	N/A
This work	6.3/8	111.8	< 1	0.31×0.31	18

where Ref — Reference, Notch — notch frequency, λ_g — guided wavelength, IL — Insertion loss, Suppression — upper stopband attenuation.

6. CONCLUSION

The single and dual notch UWB BPFs are developed by placing a stub-loaded resonator inside UWB BPF with consideration of two parallel transmission paths. The stub-loaded resonator creates notches in the passband to eliminate the interference from WLAN and satellite communication systems. There is flexibility in placing the notch frequency at the points of interest by varying the length of stub-loaded resonator. All the filters are fabricated on Rogers R03010 with relative permittivity of 10.2 and substrate thickness of 1.28 mm. The proposed filter achieves reasonable agreement between simulated and measured results. The proposed filters exhibit good performances in terms of 3-dB fractional bandwidth, compact size and selectivity.

REFERENCES

1. Mahttei, G., L. Young, and E. M. T. Jones, *Microwave Filters, Impedance Matching Networks and Coupling Structure*, Artech House, Norwood, MA, 1980.
2. Federal Communications Commission, “Revision of part 15 of the commission’s rules regarding ultra-wideband transmission systems,” Tech. Rep., ET-Docket 98–153, FCC02–48, Apr. 2002.
3. Zhu, L., S. Sun, and W. Menzel, “Ultra-wideband (UWB) bandpass filters using multiple-mode resonator,” *IEEE Microwave and Wireless Components Letters*, Vol. 15, No. 11, 796–798, Nov. 2005.
4. Feng, W., W. Che, and Q. Xue, “Compact ultra-wideband bandpass filters with narrow notched bands based on a ring resonator,” *IET Microwaves, Antennas & Propagation*, Vol. 7, No. 12, 961–969, Sept. 17, 2013.

5. Sarkar, P., R. Ghatak, M. Pal, and D. R. Poddar, "High-selective compact UWB bandpass filter with dual notch bands," *IEEE Microwave and Wireless Components Letters*, Vol. 24, No. 7, 448–450, Jul. 2014.
6. Deng, H. W., Y. Zhao, Y. He, S. L. Jia, and M. Wang, "Compact dual-notched balanced UWB BPF with folded triple-mode slotline resonator," *Electronics Letters*, Vol. 50, No. 6, 447–449, Mar. 13, 2014.
7. Lee, C. H., C. I. G. Hsu, and C. J. Chen, "Band-notched balanced UWB BPF with stepped-impedance slotline multi-mode resonator," *IEEE Microwave and Wireless Components Letters*, Vol. 22, No. 4, 182–184, Apr. 2012.
8. Mirzaee, M. and B. S. Virdee, "UWB bandpass filter with notch-band based on transversal signal-interaction concepts," *Electronics Letters*, Vol. 49, No. 6, 399–401, Mar. 14, 2013.
9. Hong, J. S. and M. J. Lancaster, *Microwave Filters for RF/Microwave Applications*, John Wiley & Sons, New York, 2001.
10. Sarkar, P., B. V. Koti Reddy, M. Pal, and R. Ghatak, "UWB bandpass filter with broad notch band and ultra-wide upper stopband," *IEEE MTT-S International Microwave and RF Conference*, 1–3, New Delhi, 2013.
11. Pirani, S., J. Nourinia, and C. Ghobadi, "Band-notched UWB BPF design using parasitic coupled line," *IEEE Microwave and Wireless Components Letters*, Vol. 20, No. 8, 444–446, Aug. 2010.
12. Xu, W., W. Kang, and C. Miao, "Compact UWB bandpass filter with a notched band using radial stub loaded resonator," *IEEE Microwave and Wireless Components Letters*, Vol. 22, No. 7, 351–353, Jul. 2012.
13. Xu, J., W. Kang, C. Miao, and W. Wu, "Sharp rejection UWB bandpass filter with notched band," *Electronics Letters*, Vol. 48, No. 16, 1005–1006, Aug. 2, 2012.
14. Li, J., C. Ding, F. Wei, and X. Wei Shi, "Compact UWB BPF with notch band based on SW-HMSIW," *Electronics Letters*, Vol. 51, No. 17, 1338–1339, Aug. 20, 2015.
15. Song, Y., G. M. Yang, and W. Geyi, "Compact UWB bandpass filter with dual notched bands using defected ground structures," *IEEE Microwave and Wireless Components Letters*, Vol. 24, No. 4, 230–232, Apr. 2014.
16. Luo, X., J. G. Ma, K. S. Yeo, and E. P. Li, "Compact ultra-wideband (UWB) bandpass filter with ultra-narrow dual- and quad-notched bands," *IEEE Transactions on Microwave Theory and Techniques*, Vol. 59, No. 6, 1509–1519, Jun. 2011.
17. Sarkar, P., R. Ghatak, M. Pal, and D. R. Poddar, "Compact UWB bandpass filter with dual notch bands using open circuited stubs," *IEEE Microwave and Wireless Components Letters*, Vol. 22, No. 9, 453–455, Sep. 2012.
18. Zhao, J., J. Wang, G. Zhang, and J. L. Li, "Compact microstrip UWB bandpass filter with dual notched bands using E-shaped resonator," *IEEE Microwave and Wireless Components Letters*, Vol. 23, No. 12, 638–640, Dec. 2013.